



OCTOBER 08 2025

Angle-of-arrival fluctuations in a turbulent atmosphere

Vladimir E. Ostashev ; Michael B. Muhlestein; D. Keith Wilson; Sergey N. Vecherin; Michelle L. Eggleston; Matthew J. Kamrath; Kent L. Gee 



J. Acoust. Soc. Am. 158, 2714–2722 (2025)

<https://doi.org/10.1121/10.0039516>



Articles You May Be Interested In

Discussion of sound propagation through the turbulent Martian atmosphere and implications for inference of turbulence spectra

J. Acoust. Soc. Am. (August 2024)

Vertical and slanted sound propagation in the near-ground atmosphere: Coherence and distributions

J. Acoust. Soc. Am. (October 2021)

Direct measurement of the inertial-convective subrange above ocean surface waves

Physics of Fluids (February 2024)



ACOUSTIC TEST CHAMBERS
FROM THE ACOUSTIC EXPERTS

COMMITTED TO A SMARTER,
MORE CONNECTED FUTURE

 **ETS-LINDGREN**
An ESCO Technologies Company

Angle-of-arrival fluctuations in a turbulent atmosphere

Vladimir E. Ostashev,^{1,a)} Michael B. Muhlestein,¹ D. Keith Wilson,¹ Sergey N. Vecherin,¹
Michelle L. Eggleston,² Matthew J. Kamrath,¹ and Kent L. Gee²

¹U.S. Army Engineer Research and Development Center, 72 Lyme Road, Hanover, New Hampshire 03755, USA

²Brigham Young University, Provo, Utah 84602, USA

ABSTRACT:

Atmospheric turbulence causes fluctuations in the angle-of-arrival (AOA) of sound waves. These fluctuations adversely affect the performance of sensor arrays used for source detection, ranging, and recognition. This article examines, from a theoretical perspective, the variance of the AOA fluctuations measured with two microphones. The AOA variance is expressed in terms of the propagation range, transverse distance between two microphones, acoustic frequency, and effective spectrum of quasi-homogeneous and isotropic turbulence, with parameters dependent upon the height above the ground. The effective spectrum is modeled with the von Kármán and Kolmogorov spectral models. In the latter case, the results simplify significantly, and the variance depends on the path-averaged effective structure-function parameter, which characterizes the intensity of temperature and wind velocity fluctuations in the inertial subrange of turbulence. The standard deviation of the AOA fluctuations is studied numerically for typical meteorological regimes of the daytime atmospheric boundary layer. For the cases considered, the standard deviation varies from a fraction of degree to around 1° – 2° , and increases with increasing friction velocity and surface heat flux. Published 2025. This is a work of the U.S. Government and is not subject to copyright protection in the United States. <https://doi.org/10.1121/10.0039516>

(Received 15 June 2025; revised 25 August 2025; accepted 12 September 2025; published online 8 October 2025)

[Editor: Didier Dragna]

Pages: 2714–2722

I. INTRODUCTION

Sound waves in the atmospheric boundary layer (ABL) are significantly affected by turbulence. The turbulence causes variations in the amplitude and phase fluctuations of acoustic signals, coherence loss, and scattering at large angles. These phenomena have been studied in the literature, e.g., Refs. 1–3 and references therein, and are important in practical applications such as source localization,⁴ auralization of flying aircraft,^{5–7} sonic boom propagation,^{8–10} sound propagation in the near-ground atmosphere,¹¹ and acoustic remote sensing of the atmosphere with sodars (sonic detection and ranging).¹²

Turbulence also causes random refraction of sound, which leads to fluctuations in the angle-of-arrival (AOA) that can be observed on sensor arrays. This phenomenon has been investigated experimentally.^{13–16} The AOA fluctuations impose performance bounds on the acoustic sensor arrays for source detection, ranging, and recognition.^{17,18}

The main goal of the present article is to formulate the AOA variance of a spherical monochromatic sound wave in a turbulent atmosphere. The AOA fluctuations depend on the microphone geometry and signal processing algorithm. Here, we assume that the phase of an incoming sound wave is measured with two microphones, i.e., with an acoustic interferometer. In this case, the AOA variance is proportional to the structure function of the acoustic phase fluctuations.

Using this approach, the AOA variance is expressed in terms of parameters of the problem, such as the propagation range, distance between two microphones, acoustic frequency, and effective spectrum of the turbulence, which is assumed here to be statistically quasi-homogeneous and isotropic. Then, the AOA variance is specified for the von Kármán and Kolmogorov effective spectra. The latter leads to a significantly simpler formulation. These new results and turbulence models in the ABL from Ref. 3 are then used to study the standard deviation of the AOA fluctuations for typical daytime meteorological regimes of the ABL.

With this Introduction, the remaining part of the article is organized as follows. Section II explains the geometry of the problem and expresses the AOA variance in terms of the structure function of the phase fluctuations. In Sec. III, the variance of the AOA fluctuations is formulated for the von Kármán and Kolmogorov effective spectra. Section IV numerically analyzes the AOA standard deviation for different meteorological conditions in the ABL. Results are summarized in Sec. V. The Appendix presents the derivation of the AOA variance of a plane sound wave.

II. VARIANCE OF THE AOA FLUCTUATIONS

A. Geometry of the problem

Let us consider AOA fluctuations for a plane monochromatic sound wave incident on two microphones at the points A and B, see Fig. 1. The Cartesian coordinates of

^{a)}Email: vladimir.ostashev@colorado.edu

the microphones are \mathbf{R}_A and \mathbf{R}_B , respectively, and the distance between them is denoted $d = |\mathbf{R}_A - \mathbf{R}_B|$. The solid lines with arrows (which are parallel) indicate the direction of sound propagation at the points A and B. Point C is a projection of point A on one of these lines so that the dashed line connecting points A and C is perpendicular to the solid lines with arrows. The angle between the propagation direction and the dashed line connecting two microphones is denoted θ .

With this geometry, the difference in the phase ϕ of the sound wave at the points B and A is given by

$$\phi(\mathbf{R}_B) - \phi(\mathbf{R}_A) = kd \cos \theta, \quad (1)$$

where k is the sound wavenumber. In the right-hand side of this equation, $d \cos \theta$ can be recognized as the distance between points C and B in Fig. 1.

Equation (1) is valid in a non-turbulent atmosphere. It is also valid approximately in a turbulent atmosphere if we ignore the phase change *due to turbulence* along the path from C to B. In a turbulent atmosphere, the phase of a sound wave $\phi(\mathbf{R})$ becomes a random field; it can be written as $\phi(\mathbf{R}) = \phi_0(\mathbf{R}) + \tilde{\phi}(\mathbf{R})$, where ϕ_0 is the mean value of the phase and $\tilde{\phi}$ is the phase fluctuation from that mean value. Similarly, $\theta = \theta_0 + \tilde{\theta}$, where θ_0 is the mean value of the propagation angle and $\tilde{\theta}$ is the AOA fluctuation. Substituting these results into Eq. (1), assuming that $|\tilde{\theta}| \ll \theta_0$, and keeping terms of order $\tilde{\phi}$ and $\tilde{\theta}$ yields

$$\tilde{\theta} = \frac{\tilde{\phi}(\mathbf{R}_A) - \tilde{\phi}(\mathbf{R}_B)}{kd \sin \theta_0}. \quad (2)$$

This formula expresses the AOA fluctuation in terms of the phase fluctuations in a plane wave at the points A and B. Equation (2) also describes the AOA fluctuation of a spherical wave, provided that the distance to the point source is much larger than d . Indeed, for such geometry, the angles θ at the points A and B differ only slightly, and the wavefront deviates insignificantly from the dashed line in Fig. 1.

Equation (2) is applicable only to the direct path from the source to the microphones. In outdoor applications, there might also be the ground-reflected path. In some cases, the latter path can be eliminated by beamforming.

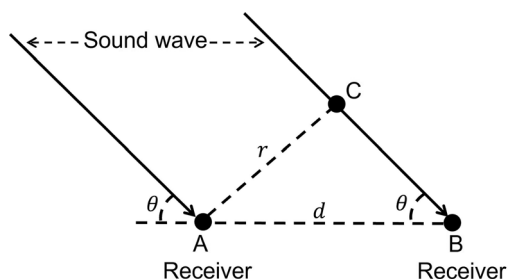


FIG. 1. Geometry of the AOA fluctuations.

B. AOA variance

The variance of the AOA fluctuations, $\sigma_{\tilde{\theta}}^2$, is obtained by squaring both sides of Eq. (2) and averaging over an ensemble of turbulence realizations. The result is

$$\sigma_{\tilde{\theta}}^2 = \langle \tilde{\theta}^2 \rangle = \frac{D_{\phi}(L; \mathbf{R}_A - \mathbf{R}_B)}{k^2 d^2 \sin^2 \theta_0}. \quad (3)$$

Here, the brackets $\langle \rangle$ denote ensemble averaging and $D_{\phi}(L; \mathbf{R}_A - \mathbf{R}_B) = \langle [\tilde{\phi}(\mathbf{R}_A) - \tilde{\phi}(\mathbf{R}_B)]^2 \rangle$ is the structure function of phase fluctuations between two observation points. The first argument L in the structure function is the propagation range of the sound wave. Equation (3) is known in electromagnetic wave propagation, e.g., Refs. 19–21; the derivation of this equation is presented here for completeness. The phase structure functions for electromagnetic and acoustic waves generally differ because the former is affected by scalar random fields (temperature and humidity fluctuations), while the latter is affected both by scalar and vector random fields (temperature and wind velocity fluctuations). For details, see Part II in Ref. 3.

The decorrelation of the phase fluctuations along the direction of sound propagation is much less than in the transverse direction.²² Therefore, the phase structure function calculated at points A and B is approximately equal to that calculated at points A and C; that is, $D_{\phi}(L; \mathbf{R}_A - \mathbf{R}_B) \approx D_{\phi}(L; \mathbf{R}_A - \mathbf{R}_C)$. The latter structure function is termed the *transverse structure function* (points A and C are in the plane perpendicular to the propagation direction). Hereinafter, we consider statistically isotropic turbulence, for which the transverse structure function depends only on the magnitude of its second argument and can be written as $D_{\phi}(L; r)$, where $r = d \sin \theta_0 = |\mathbf{R}_A - \mathbf{R}_C|$ is the distance between the points A and C. The distance r can also be termed the transverse distance between the points A and B. With these results, Eq. (3) takes the form

$$\sigma_{\tilde{\theta}}^2 = \frac{D_{\phi}(L; r)}{k^2 r^2}. \quad (4)$$

This formula expresses the AOA variance in terms of the transverse phase structure function. The dependence of $\sigma_{\tilde{\theta}}^2$ on r is determined by the dependence of $D_{\phi}(L; r)$ on r . Equation (4) is valid for both plane and spherical propagation. The former case corresponds to a point sound source located significantly above the ABL and is considered in the Appendix. Spherical propagation is attained when a point source is located within the ABL. Unless stated otherwise, a spherical wave is considered in the remaining part of this article.

The phase structure function can be written as (e.g., Refs. 3 and 19)

$$D_{\phi}(L; r) = 2[B_{\phi}(L; 0) - B_{\phi}(L; r)], \quad (5)$$

where $B_{\phi}(L; r) = \langle \tilde{\phi}(\mathbf{R}_A) \tilde{\phi}(\mathbf{R}_C) \rangle$ is the correlation function of the phase fluctuations. For anisotropic turbulence, the

phase correlation function of a spherical wave is given by Eq. (7.95) in Ref. 3. For isotropic turbulence, the two-dimensional integral over the transverse turbulence wave vector in that equation can be reduced to a one-dimensional integral. Substituting the result into Eq. (5) yields

$$D_\phi(L; r) = \pi^2 k^2 L \int_0^1 d\eta \int_0^\infty \Phi_{\text{eff}}(\eta L; \kappa) [1 - J_0(\eta \kappa r)] \times \left[1 + \cos\left(\frac{\eta(1-\eta)\kappa^2 L}{k}\right) \right] \kappa d\kappa. \quad (6)$$

Here, J_0 is the Bessel function of the first kind of zero order and κ is the turbulence wavenumber, which is inversely proportional to the scale l of turbulent eddies, i.e., $\kappa \sim 1/l$. In Eq. (6), the integral over η corresponds to integration along the normalized sound propagation path from the point source to the center between points A and C in Fig. 1. Furthermore, $\Phi_{\text{eff}}(\eta L; \kappa)$ is the *effective spectrum* of turbulence, which accounts for both temperature and velocity fluctuations. The effective spectrum is explained in detail in Refs. 3, 23, and 24 and is specified in Sec. III A for the von Kármán and Kolmogorov spectral models. The first argument ηL in the effective spectrum indicates that the parameters of $\Phi_{\text{eff}}(\eta L; \kappa)$ can vary gradually along the propagation path; this assumption corresponds to propagation through statistically *quasi-homogeneous* turbulence. For statistically homogeneous turbulence, Φ_{eff} remains constant along the path and Eq. (6) coincides with Eq. (7.101) in Ref. 3. Note that Eq. (6) is still valid even if $B_\phi(L; 0)$ does not exist because it can be derived without using Eq. (5).³

If $\kappa r \ll 1$, the difference $1 - J_0(\eta \kappa r)$ in Eq. (6) is small compared to 1. This means that turbulent eddies with $\kappa \ll 1/r$, or equivalently $l \gg r$, do not contribute significantly to the phase structure function. Since Φ_{eff} decreases rapidly with increasing κ [see Eqs. (8) and (13)], turbulent eddies with $l \ll r$ (or $\kappa \gg 1/r$) also do not contribute to $D_\phi(L; r)$. Thus, the phase structure function is mainly affected by turbulent eddies with scales $l \sim r$.

Another important consideration is that Eq. (7.95) in Ref. 3 and Eq. (6) in the present article are derived assuming that random inhomogeneities with scales $l \lesssim \lambda$, where λ is the sound wavelength, do not significantly affect the phase structure function. This implies that Eq. (6) is valid only if the transverse distance between two microphones is greater than the wavelength, i.e., $r \gtrsim \lambda$.

Substituting Eq. (6) into Eq. (4) yields

$$\sigma_\theta^2 = \frac{\pi^2 L}{r^2} \int_0^1 d\eta \int_0^\infty \Phi_{\text{eff}}(\eta L; \kappa) [1 - J_0(\eta \kappa r)] \times \left[1 + \cos\left(\frac{\eta(1-\eta)\kappa^2 L}{k}\right) \right] \kappa d\kappa. \quad (7)$$

This formula expresses the AOA variance of a spherical wave propagating through quasi-homogeneous and isotropic turbulence in terms of the propagation range (L), transverse distance between two microphones (r), sound wavenumber (k), and effective spectrum of turbulence (Φ_{eff}). Similar to

the phase structure function, σ_θ^2 is affected by turbulent eddies with scales $l \sim r$ and is valid if $r \gtrsim \lambda$.

III. VARIANCE IN THE ABL

In this section, the AOA variance is calculated for sound propagation in the ABL when parameters of the effective spectrum Φ_{eff} depend on the height z above the ground.

A. Effective turbulence spectra

1. von Kármán effective spectrum

The von Kármán effective spectrum accounts for temperature and velocity fluctuations in the inertial and energy-containing subranges of turbulence and has been used in a number of recent studies.^{4–6,23,24} This spectrum is given by³

$$\Phi_{\text{eff}}^{\text{vK}}(z; 0, \kappa) = \frac{\Gamma(11/6)}{\pi^{3/2}\Gamma(1/3)} \left[\frac{\sigma_T^2(z) L_T^3(z)}{T_0^2 (1 + \kappa^2 L_T^2(z))^{11/6}} + \frac{22}{3} \frac{\sigma_{v,s}^2 L_{v,s}^5(z) \kappa^2}{c_0^2 (1 + \kappa^2 L_{v,s}^2(z))^{17/6}} + \frac{22}{3} \frac{\sigma_{v,b}^2 L_{v,b}^5(z) \kappa^2}{c_0^2 (1 + \kappa^2 L_{v,b}^2(z))^{17/6}} \right], \quad (8)$$

where Γ is the gamma function, and T_0 , c_0 are the mean temperature and sound speed. Moreover, $\sigma_T^2(z)$, $\sigma_{v,s}^2$, and $\sigma_{v,b}^2$ are the variances of the temperature fluctuations, shear-produced velocity fluctuations, and buoyancy-produced velocity fluctuations, respectively, and $L_T(z)$, $L_{v,s}(z)$, and $L_{v,b}$ are the corresponding outer scales. Some variances and outer scales depend on z , while others do not. Section 6.2.4 in Ref. 3 expresses these variances and scales in terms of the meteorological parameters of the ABL,

$$\sigma_T^2(z) = \frac{4.0 T_*^2}{(1 - 10z/L_o)^{2/3}}, \quad \sigma_{v,s}^2 = 3.0 u_*^2, \quad \sigma_{v,b}^2 = 0.35 w_*^2, \quad (9)$$

$$L_T(z) = 2.0 z \frac{1 - 7.0z/L_o}{1 - 10z/L_o}, \quad L_{v,s}(z) = 1.8 z, \quad L_{v,b} = 0.23 z_i. \quad (10)$$

Here, u_* is the friction velocity and z_i is the ABL height. In Eqs. (9) and (10), L_o is the Obukhov length, T_* is the surface-layer temperature scale, and w_* is the mixed-layer velocity scale, which are defined by the following equations:

$$L_o = -\frac{c_P \rho_a T_s u_*^3}{\kappa_v g Q_H}, \quad T_* = -\frac{Q_H}{\rho_a c_P u_*}, \quad w_* = \left(\frac{g z_i Q_H}{\rho_a c_P T_s} \right)^{1/3}. \quad (11)$$

In these formulas, c_P is the specific heat of air at constant pressure, ρ_a is the air density, T_s is the air temperature near the ground, $\kappa_v = 0.40$ is the von Kármán constant, g is the gravitational acceleration, and Q_H is the surface sensible heat flux.

Equations (9)–(11) express the variances and outer scales of temperature and velocity fluctuations in the von Kármán effective spectrum $\Phi_{\text{eff}}^{\text{VK}}(z; \kappa)$ in terms of the meteorological parameters of the ABL. The dependence of $\Phi_{\text{eff}}^{\text{VK}}(z; \kappa)$ on the height z corresponds to statistical quasi-homogeneity.

2. Kolmogorov effective spectrum

In practical applications, the transverse distance r between two microphones is usually on the order of a meter. On the other hand, the outer scales $L_T(z)$ and $L_{v,s}(z)$ increase approximately linearly with the height z , while $L_{v,b}$ does not depend on z and is greater than 100 m for a typical ABL. Therefore, in many applications,

$$r \ll L_T(z), \quad L_{v,s}(z), \quad L_{v,b}. \quad (12)$$

Here, the first two inequalities are considered for horizontal sound propagation, when $L_T(z)$ and $L_{v,s}(z)$ are constant along the path. For vertical and slanted propagation, z in Eq. (12) should be replaced with a weighted average height along the propagation path.

If the inequalities in Eq. (12) are fulfilled, the AOA variance is affected mainly by eddies in the inertial subrange of turbulence with scales $l \ll L_T, L_{v,s}, L_{v,b}$. For such eddies, $\kappa L_T \gg 1$, $\kappa L_{v,s} \gg 1$, and $\kappa L_{v,b} \gg 1$ in the von Kármán effective spectrum given by Eq. (8). In this case, the von Kármán spectrum simplifies significantly and reduces to the Kolmogorov spectrum,^{3,25}

$$\Phi_{\text{eff}}^{\text{K}}(z; \kappa) = Q C_{\text{eff}}^2(z) \kappa^{-11/3}. \quad (13)$$

Here, $Q = 5/[18\pi\Gamma(1/3)] \approx 0.0330$ is a numerical coefficient and C_{eff}^2 is the *effective structure-function parameter*,

$$C_{\text{eff}}^2(z) = \frac{C_T^2(z)}{T_0^2} + \frac{22}{3} \frac{C_{v,s}^2(z)}{c_0^2} + \frac{22}{3} \frac{C_{v,b}^2}{c_0^2}. \quad (14)$$

In this formula, C_T^2 , $C_{v,s}^2$, and $C_{v,b}^2$ are the structure-function parameters of the temperature fluctuations, shear-produced velocity fluctuations, and buoyancy-produced velocity fluctuations, which characterize the intensity of the corresponding fluctuations in the inertial subrange. They are given by

$$C_T^2(z) = \frac{3\Gamma(5/6)}{\sqrt{\pi}} \frac{\sigma_T^2(z)}{L_T^{2/3}(z)}, \quad C_{v,s}^2(z) = \frac{3\Gamma(5/6)}{\sqrt{\pi}} \frac{\sigma_{v,s}^2}{L_{v,s}^{2/3}(z)},$$

$$C_{v,b}^2 = \frac{3\Gamma(5/6)}{\sqrt{\pi}} \frac{\sigma_{v,b}^2}{L_{v,b}^{2/3}}. \quad (15)$$

Replacing the variances and outer scales in these formulas with Eqs. (9) and (10) yields

$$C_T^2(z) = \frac{2.5 A T_*^2}{z^{2/3} [1 + (1 - 7.0 z/L_o)]^{2/3}},$$

$$C_{v,s}^2(z) = \frac{2.0 A u_*^2}{z^{2/3}}, \quad C_{v,b}^2 = 0.93 A \left(\frac{g Q_H}{\rho_a c_P T_s} \right)^{2/3}, \quad (16)$$

where $A = 3\Gamma(5/6)/\sqrt{\pi} \approx 1.9$ is a numerical coefficient. Equation (16) determines C_T^2 , $C_{v,s}^2$, and $C_{v,b}^2$ in terms of meteorological parameters of the ABL. It follows from this equation that C_T^2 and $C_{v,s}^2$ decrease with increasing height z , while $C_{v,b}^2$ remains constant.

B. AOA variance

1. Von Kármán effective spectrum

Substituting Eq. (8) into Eq. (7) yields the AOA variance of a spherical wave for the von Kármán effective spectrum

$$\sigma_\theta^2 = \frac{\sqrt{\pi}\Gamma(11/6)L}{\Gamma(1/3)r^2} \int_0^1 d\eta \int_0^\infty \left[\frac{\sigma_T^2(\tilde{z}) L_T^3(\tilde{z})}{T_0^2 (1 + \kappa^2 L_T^2(\tilde{z}))^{11/6}} + \frac{22}{3} \frac{\sigma_{v,s}^2 L_{v,s}^5(\tilde{z}) \kappa^2}{c_0^2 (1 + \kappa^2 L_{v,s}^2(\tilde{z}))^{17/6}} + \frac{22}{3} \frac{\sigma_{v,b}^2 L_{v,b}^5 \kappa^2}{c_0^2 (1 + \kappa^2 L_{v,b}^2)^{17/6}} \right]$$

$$\times [1 - J_0(\eta \kappa r)] \left[1 + \cos\left(\frac{\eta(1 - \eta) \kappa^2 L}{k}\right) \right] \kappa d\kappa. \quad (17)$$

Here, the function $\tilde{z} = \tilde{z}(\eta L)$ in the arguments of the variances and outer scales of temperature and velocity fluctuations returns the height above the ground along the propagation path. This function depends on the geometry of sound propagation. For horizontal propagation at the height h ,

$$\tilde{z}(\eta L) = h. \quad (18)$$

For sound propagation from an elevated source to the microphones on the ground,

$$\tilde{z}(\eta L) = (1 - \eta) h_s. \quad (19)$$

In this formula, $h_s = L \cos \alpha$ is the source height, where α is the angle between the propagation path and vertical. The case $\alpha = 0$ corresponds to vertical propagation. Finally, for sound propagation from a ground-based source to the elevated microphones

$$\tilde{z}(\eta L) = \eta h_r, \quad (20)$$

where $h_r = L \cos \alpha$ is the microphones' height.

2. Kolmogorov effective spectrum

Substituting Eq. (13) into Eq. (7) and setting $\kappa = \xi/(\eta r)$, where ξ is a new non-dimensional integration variable, we obtain the AOA variance of a spherical wave for the Kolmogorov spectral model,

$$\sigma_\theta^2 = \frac{\pi^2 Q L}{r^{1/3}} \int_0^1 d\eta \eta^{5/3} C_{\text{eff}}^2(\tilde{z}) \int_0^\infty [1 - J_0(\xi)] \times [1 + \cos((1/\eta - 1)\xi^2 \mu)] \xi^{-8/3} d\xi. \quad (21)$$

Here, $\tilde{z} = \tilde{z}(\eta L)$ is the same function as in Eq. (17) and μ is the parameter given by

$$\mu = \frac{L}{kr^2}. \quad (22)$$

The square root $\sqrt{\mu}$ can be recognized as the ratio between the first Fresnel zone $\sqrt{L/k}$ and the transverse distance r . Therefore, the parameter μ in Eq. (21) characterizes the diffraction regime of the considered problem. There are two limiting diffraction regimes. The first is geometrical acoustics (weak diffraction), which is attained when the diffraction parameter $\mu \ll \pi/2$. In this case, the argument of the cosine function in Eq. (21) is small compared to $\pi/2$, and this function can be set to 1. The other limiting case is Fraunhofer (strong) diffraction when $\mu \gg \pi/2$, the cosine function oscillates rapidly, and does not contribute to σ_θ^2 . In both limiting diffraction regimes, the two-dimensional integral in Eq. (21) becomes a product of one-dimensional integrals over η and ξ . The former integral yields the path-averaged effective structure-function parameter,

$$\bar{C}_{\text{eff}}^2 = \frac{8}{3} \int_0^1 C_{\text{eff}}^2(\tilde{z}(\eta L)) \eta^{5/3} d\eta. \quad (23)$$

In this formula, the coefficient $8/3$ is introduced as a normalization factor and $\eta^{5/3}$ in the integrand is a weight function along the propagation path. The integral over ξ can be calculated analytically using Eq. (10) on page 407 in Ref. 19, with the result

$$\int_0^\infty [1 - J_0(\xi)] \xi^{-8/3} d\xi = \frac{3\Gamma(1/6)}{2^{5/3}5\Gamma(11/6)}. \quad (24)$$

With these transformations, Eq. (21) reads

$$\sigma_\theta^2 = \frac{B\beta_0 \bar{C}_{\text{eff}}^2 L}{r^{1/3}}. \quad (25)$$

Here, $B = 3\sqrt{\pi}\Gamma(1/6)/(2^{5/3}5\Gamma(2/3)) \approx 0.137$ is a numerical coefficient, $\beta_0 = 2$ in geometrical acoustics, and $\beta_0 = 1$ in Fraunhofer diffraction. Equation (25) provides a remarkably simple formula for the AOA variance, which depends on the propagation range (L), the transverse distance between two microphones (r), and the turbulence intensity in the inertial sub-range (\bar{C}_{eff}^2). In geometrical acoustics, the dependence of σ_θ^2 on L and r was also predicted in Ref. 26, see Sec. 11 in Ref. 27.

For horizontal sound propagation, $C_{\text{eff}}^2(h)$ remains constant along the path. In this case, it follows from Eq. (23) that $\bar{C}_{\text{eff}}^2 = C_{\text{eff}}^2(h)$. Furthermore, Eq. (21) can be written as

$$\sigma_\theta^2 = \frac{B\beta(\mu)C_{\text{eff}}^2(h)L}{r^{1/3}}, \quad (26)$$

where β is a function of μ given by

$$\beta(\mu) = \frac{\pi^2 Q}{B} \int_0^1 d\eta \eta^{5/3} \int_0^\infty [1 - J_0(\xi)] \times [1 + \cos((1/\eta - 1)\xi^2 \mu)] \xi^{-8/3} d\xi. \quad (27)$$

It can be shown that $\beta = 2$ if $\mu \ll \pi/2$ and $\beta = 1$ if $\mu \gg \pi/2$. Therefore, in these limiting cases, Eq. (27) is consistent with Eq. (25).

Note that in the limiting cases of geometrical acoustics and Fraunhofer diffraction, the cosine function in Eq. (17) for the von Kármán spectrum can also be set to 1 and 0, respectively. However, unlike the Kolmogorov spectrum, the two-dimensional integral over η and κ in Eq. (17) does not become a product of one-dimensional integrals.

IV. NUMERICAL RESULTS

In this section, the standard deviation of the AOA fluctuations $\sigma_\theta = \sqrt{\sigma_\theta^2}$ is studied numerically for horizontal sound propagation at the height h above the ground. It is assumed that the transverse distance between two microphones is $r = 1$ m, the acoustic frequency is $f = kc_0/(2\pi) = 1$ kHz, the air temperature is $T_0 = T_s = 20^\circ\text{C}$, and the ABL height is $z_i = 1$ km.

The solid and dashed black lines in Fig. 2 depict the AOA standard deviation σ_θ for the von Kármán and Kolmogorov effective spectra versus the propagation range L . The results are obtained with Eqs. (17) and (26) and correspond to the sound propagation height $h = 20$ m, $u_* = 0.6$ m/s (which is representative of strong wind), and $Q_H = 400$ W/m² (sunny conditions). These parameters enable us to calculate the variances and outer scales of temperature and wind velocity fluctuations in the von Kármán effective spectrum and the effective structure-function parameter in the Kolmogorov spectrum. In Fig. 2, the maximum values of σ_θ are 2.1° for the von Kármán spectrum and 2.4° for the Kolmogorov spectrum. At the range of 500 m, these values correspond to an apparent source displacement of 18.3 and 20.9 m, respectively.

The blue and red dash-dotted lines in Fig. 2 depict the dependence of σ_θ on L attained for the Kolmogorov spectrum in geometrical acoustics and Fraunhofer diffraction,

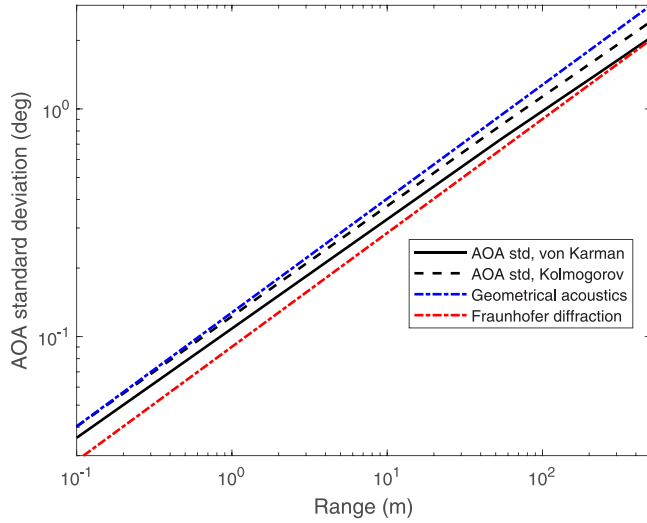


FIG. 2. Standard deviation of the AOA fluctuations versus range for $u_* = 0.6$ m/s, $Q_H = 400$ W/m², and horizontal sound propagation at the height $h = 20$ m. The solid and dashed black lines correspond to the von Kármán and Kolmogorov effective spectra, respectively. The blue and red dash-dotted lines respectively correspond to geometrical acoustics and Fraunhofer diffraction.

when $\beta(\mu)$ in Eq. (26) equals 2 and 1, respectively. For the considered parameters of the calculations, the diffraction parameter μ varies between 0.0055 (for $L = 0.1$ m) and 27.3 (for $L = 500$ m). As a result, for relatively small propagation ranges, σ_θ for the Kolmogorov spectrum is close to that in geometrical acoustics. For large propagation ranges, σ_θ starts to deviate from the geometrical acoustics results and gradually approaches the Fraunhofer diffraction limit.

It follows from Fig. 2 that the dashed black line is between the blue and red dash-dotted lines. Therefore, in some cases, σ_θ for the Kolmogorov spectrum can be approximated as the mean of the AOA standard deviations in geometrical acoustics and Fraunhofer diffraction, which is given by

$$\sigma_\theta = \frac{1 + \sqrt{2}}{2} \frac{[BC_{\text{eff}}^2(h)L]^{1/2}}{r^{1/6}}. \quad (28)$$

The maximum relative difference between σ_θ given by Eq. (28) and that for the Kolmogorov spectrum is 17%. With this accuracy, σ_θ for the Kolmogorov spectrum [Eq. (28)] depends on the propagation range and transverse microphone separation as $L^{1/2}/r^{1/6}$ and does not depend on frequency.

The AOA standard deviation σ_θ for the von Kármán spectrum in Fig. 2 is close to that for the Kolmogorov spectrum and is also between the blue and red dash-dotted lines. The maximum relative difference between σ_θ for two spectra is 18%. This relatively small difference is due to the fact that, in the considered case, the transverse distance between two microphones $r = 1$ m is much smaller than the outer scales $L_T = 30.4$ m, $L_{v,s} = 36$ m, and $L_{v,b} = 230$ m of temperature and velocity fluctuations so that the inequalities in Eq. (12) are fulfilled.

Figure 3 depicts the AOA standard deviation versus the surface heat flux Q_H for three values of the friction velocity corresponding to light ($u_* = 0.1$ m/s), moderate ($u_* = 0.3$ m/s),

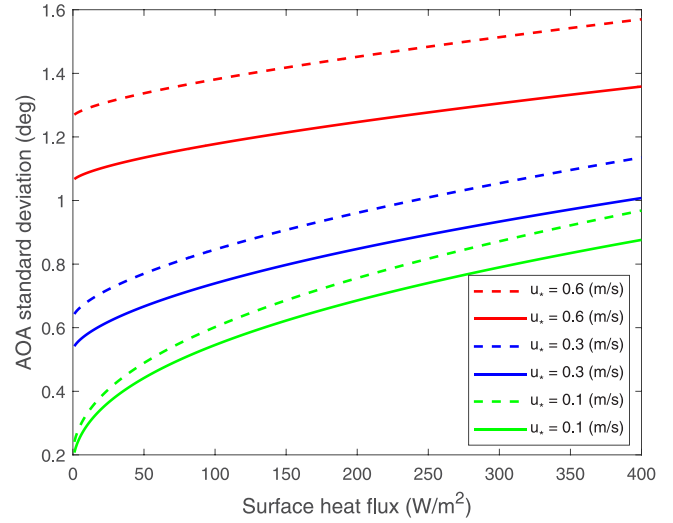


FIG. 3. Standard deviation of the AOA fluctuations versus the surface heat flux for three values of the friction velocity. The solid and dashed lines correspond to the von Kármán and Kolmogorov effective spectra, respectively.

and strong ($u_* = 0.6$ m/s) wind conditions. The limiting values of Q_H (i.e., $Q_H = 1$ W/m² and $Q_H = 400$ W/m²) are representative of cloudy and sunny conditions. In Fig. 3, the height above the ground $h = 20$ m is the same as in Fig. 2, while the propagation range is $L = 200$ m. The solid and dashed lines correspond to the results obtained with the von Kármán and Kolmogorov effective spectra, respectively.

It follows from Fig. 3 that σ_θ increases with increasing heat flux and friction velocity. The maximum values of the AOA standard deviations are 1.4° for the von Kármán spectrum and 1.6° for the Kolmogorov spectrum. The results for these spectra are close to each other; the maximum relative difference is 16% for $u_* = 0.1$ m/s and 19% for $u_* = 0.3$ m/s and $u_* = 0.6$ m/s. These small differences can again be explained by the fact that the inequalities in Eq. (12) are fulfilled: for the parameters pertinent to Fig. 3, L_T varies between 28.0 m and 39.9 m, while $L_{v,s}$ and $L_{v,b}$ are the same as in Fig. 2.

Let $\sigma_{\theta,T}$, $\sigma_{\theta,vs}$, and $\sigma_{\theta,vb}$ be the AOA standard deviations due to the temperature fluctuations, shear-produced velocity fluctuations, and buoyancy-produced velocity fluctuations, respectively. For the von Kármán spectrum, $\sigma_{\theta,T}$ is determined by setting $\sigma_{v,s}^2 = \sigma_{v,b}^2 = 0$ in Eq. (17); the standard deviations $\sigma_{\theta,vs}$ and $\sigma_{\theta,vb}$ are determined similarly. Figure 4 depicts $\sigma_{\theta,T}$, $\sigma_{\theta,vs}$, and $\sigma_{\theta,vb}$ versus the surface heat flux Q_H for moderate wind conditions ($u_* = 0.3$ m/s) and the same h and L as in Fig. 3. It follows from the figure that $\sigma_{\theta,T}$ and $\sigma_{\theta,vb}$ increase with increasing Q_H , while $\sigma_{\theta,vs}$ remains constant. The standard deviation $\sigma_{\theta,T}$ is smaller than $\sigma_{\theta,vs}$ and $\sigma_{\theta,vb}$ for all Q_H . For $Q_H > 120$ W/m², $\sigma_{\theta,vb} > \sigma_{\theta,vs}$, while the opposite inequality is valid if $Q_H < 120$ W/m². The standard deviations $\sigma_{\theta,T}$, $\sigma_{\theta,vs}$, and $\sigma_{\theta,vb}$ were also analyzed for low and strong wind conditions. For $u_* = 0.1$ m/s, $\sigma_{\theta,vb} > \sigma_{\theta,vs}$ if $Q_H > 4$ W/m². For $u_* = 0.6$ m/s, $\sigma_{\theta,vs}$ is always larger than $\sigma_{\theta,vb}$. In both wind conditions, $\sigma_{\theta,T}$ is smaller than $\sigma_{\theta,vs}$ and/or $\sigma_{\theta,vb}$.

Note that if some of the inequalities in Eq. (12) are not fulfilled, the AOA variance for the Kolmogorov spectrum

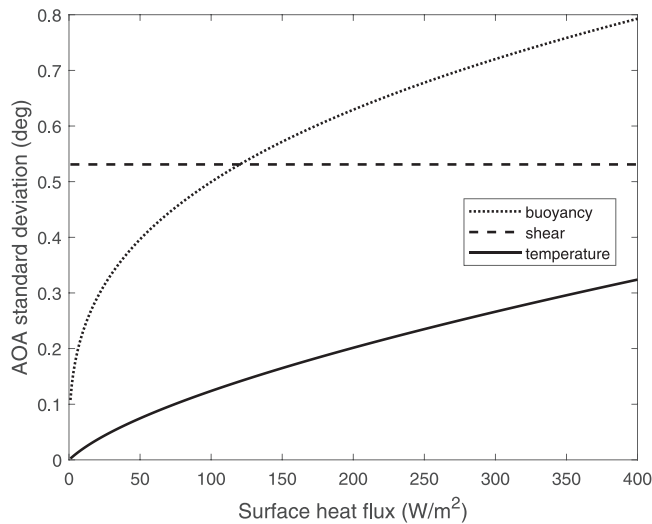


FIG. 4. Standard deviations due to the temperature fluctuations, shear-produced velocity fluctuations, and buoyancy-produced velocity fluctuations versus the surface heat flux for moderate wind conditions.

can deviate noticeably from that for the von Kármán spectrum. As an example, let us consider the same parameters of the problem as in Fig. 2 except for the height of sound propagation, which is $h = 2$ m. In this case, σ_θ versus the propagation range is depicted in Fig. 5. It follows from the figure that σ_θ for the von Kármán spectrum is noticeably smaller than that for the Kolmogorov spectrum, with the maximum relative difference of 58%. This relatively large difference is due to the fact that for $h = 2$ m, the outer scales $L_T = 3.7$ m and $L_{v,s} = 3.6$ m are comparable to the transverse distance between two microphones $r = 1$ m so that the first two inequalities in Eq. (12) are not fulfilled.

V. CONCLUSIONS

This article presented a theoretical analysis of the variance of the AOA fluctuations of a spherical sound wave in a turbulent atmosphere.

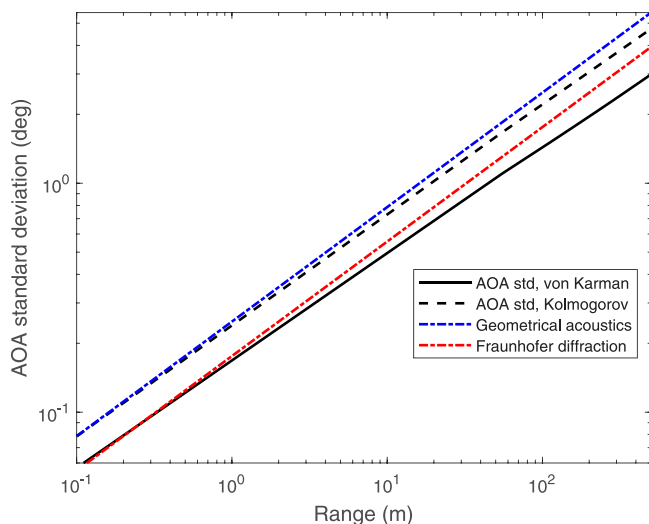


FIG. 5. Same as in Fig. 2 but for horizontal propagation at the height $h = 2$ m.

Equation (7) expressed the AOA variance in terms of the propagation range, transverse distance between two microphones, acoustic frequency, and the effective spectrum of statistically quasi-homogeneous and isotropic turbulence whose parameters can vary along the propagation path. Then, the results were specified for sound propagation in the ABL, where the effective spectrum was modeled with the von Kármán and Kolmogorov spectral models. It was argued that the latter spectrum can be used if the transverse distance between two microphones is much smaller than the outer scales of temperature and velocity fluctuations. The AOA variances for the von Kármán and Kolmogorov effective spectra given by Eqs. (17) and (21), respectively, are valid for vertical, slanted, or horizontal propagation. For the Kolmogorov spectrum, the variance is proportional to the path-averaged effective structure-function parameter, which characterizes the intensity of temperature and wind velocity fluctuations in the inertial subrange. Equations (25) and (26) provide remarkably simple expressions for the AOA variance in the limiting cases of weak/strong diffraction or statistically homogeneous turbulence and elucidate the dependence of the variance on parameters of the problem.

The standard deviation of the AOA fluctuations was analyzed numerically for various meteorological regimes of the ABL. It was shown that the standard deviation increases with increasing propagation range, surface heat flux, and friction velocity and varies in the range from a fraction of a degree to 1° – 2° . The numerical results substantiated that the AOA standard deviations for the von Kármán and Kolmogorov spectra are close to each other, provided that the transverse distance between the microphones is much smaller than the outer scales of temperature and velocity fluctuations. With the accuracy of about 17%, the AOA standard deviation for the Kolmogorov spectrum depends on the propagation range L and transverse distance r between two microphones as $L^{1/2}/r^{1/6}$ and is frequency independent.

The theoretical predictions for the AOA variance were not compared with experimental data reported in Refs. 13, 14, and 16 because the meteorological parameters necessary for such a comparison were not reported in these works. In Ref. 15, the AOA fluctuations were measured with an acoustic vector sensor, which is essentially a point sensor. The theory developed in the present article does not apply to such sensors.

The obtained results correspond to the phase fluctuations measured with two microphones. Many other acoustic sensor arrays also rely on the phase measurements of an incoming signal at different microphones. Therefore, the results of this article can provide, at least qualitatively, the dependence of the AOA variance, when measured with other sensor arrays, on parameters such as the propagation range, frequency, and turbulence intensity. For arrays with more than two sensors, the aperture across the entire array should be used instead of the transverse distance r between two microphones.

ACKNOWLEDGMENTS

This research was funded by the U.S. Army Engineer Research and Development Center (ERDC) basic research program. Permission to publish was granted by Director, Cold Regions Research and Engineering Laboratory.

AUTHOR DECLARATION

Conflict of Interest

The authors have no conflicts to disclose.

DATA AVAILABILITY

Data sharing is not applicable to this article as no new data were created.

APPENDIX: AOA VARIANCE OF A PLANE WAVE

This Appendix presents the derivation of the AOA variance of a plane sound wave.

The phase correlation function of a plane sound wave propagating through statistically quasi-homogeneous and anisotropic turbulence is given by Eq. (7.77) in Ref. 3. This equation is substituted into Eq. (5) and, for isotropic turbulence, the two-dimensional integral over the transverse turbulence wave vector is reduced to a one-dimensional integral. The result is

$$D_\phi(L; r) = \pi^2 k^2 L \int_0^1 d\eta \int_0^\infty \Phi_{\text{eff}}(\eta L; \kappa) [1 - J_0(\kappa r)] \times \left[1 + \cos\left(\frac{(1-\eta)\kappa^2 L}{k}\right) \right] \kappa d\kappa. \quad (\text{A1})$$

This formula provides the phase structure function of a plane sound wave in quasi-homogeneous and isotropic turbulence. Equation (A1) coincides with Eq. (6) for $D_\phi(L; r)$ of a spherical wave if, in the latter equation, the arguments of the Bessel and cosine functions are divided by η .

Substituting Eq. (A1) into Eq. (4) yields the AOA variance for a plane wave,

$$\sigma_\theta^2 = \frac{\pi^2 L}{r^2} \int_0^1 d\eta \int_0^\infty \Phi_{\text{eff}}(\eta L; \kappa) [1 - J_0(\kappa r)] \times \left[1 + \cos\left(\frac{(1-\eta)\kappa^2 L}{k}\right) \right] \kappa d\kappa. \quad (\text{A2})$$

The AOA variances for von Kármán and Kolmogorov effective spectra are obtained by replacing Φ_{eff} in this equation with Eqs. (8) and (13), respectively.

In the remainder of this Appendix, results pertinent to the Kolmogorov spectrum are derived. For this spectrum, introducing a new non-dimensional integration variable $\xi = \kappa r$ in Eq. (A2), we obtain the AOA variance of a plane sound wave,

$$\sigma_\theta^2 = \frac{\pi^2 Q L}{r^{1/3}} \int_0^1 d\eta C_{\text{eff}}^2(\xi(\eta L)) \int_0^\infty [1 - J_0(\xi)] \times [1 + \cos((1-\eta)\xi^2 \mu)] \xi^{-8/3} d\xi. \quad (\text{A3})$$

This equation coincides with Eq. (21) for σ_θ^2 of a spherical wave if, in the latter equation, the weight function $\eta^{5/3}$ is set to 1 and the argument of the cosine function is multiplied by η .

Similar to spherical wave propagation, geometrical acoustics is attained for $\mu \ll \pi/2$, when the cosine function in Eq. (A3) can be set to 1. In Fraunhofer diffraction, $\mu \gg \pi/2$ so that the cosine function can be approximated with 0. In these limiting cases, Eq. (A3) simplifies to

$$\sigma_\theta^2 = \frac{8 B \beta_0 \bar{C}_{\text{eff}}^2 L}{3 r^{1/3}}. \quad (\text{A4})$$

Here, the path-averaged effective structure-function parameter is given by

$$\bar{C}_{\text{eff}}^2 = \int_0^1 C_{\text{eff}}^2(\xi(\eta L)) d\eta. \quad (\text{A5})$$

Equation (A4) is similar to Eq. (25) for σ_θ^2 of a spherical sound wave except for two differences. First, \bar{C}_{eff}^2 given by Eq. (A5) does not have a weight function, while in Eq. (23) for a spherical wave, the weight function is $\eta^{5/3}$. Second, Eq. (A4) contains the additional factor 8/3 that is absent in Eq. (25) for a spherical wave. Due to this factor, the AOA variance for a plane wave is 8/3 times larger than that for a spherical wave in statistically homogeneous turbulence when $\bar{C}_{\text{eff}}^2 = C_{\text{eff}}^2$.

The case when C_{eff}^2 is constant along the propagation path can be considered similarly to Sec. III B 2.

¹V. I. Tatarskii, *The Effects of the Turbulent Atmosphere on Wave Propagation* (Israel Program for Scientific Translation, Jerusalem, Israel, 1971).

²E. H. Brown and F. F. Hall, "Advances in atmospheric acoustics," *Rev. Geophys. Space. Phys.* **16**(1), 47–100 (1978).

³V. E. Ostashev and D. K. Wilson, *Acoustics in Moving Inhomogeneous Media*, 2nd ed. (CRC Press, Boca Raton, FL, 2015).

⁴D. Lincke, T. Schumacher, and R. Pieren, "Synthesizing coherence loss by atmospheric turbulence in virtual microphone array signals," *J. Acoust. Soc. Am.* **153**, 456–466 (2023).

⁵R. Pieren and D. Lincke, "Auralization of aircraft flyovers with turbulence-induced coherence loss in ground effect," *J. Acoust. Soc. Am.* **151**, 2453–2460 (2022).

⁶A. P. C. Bresciani, J. Maillard, and L. D. de Santana, "Physics-based scintillations for outdoor sound auralization," *J. Acoust. Soc. Am.* **154**, 1179–1190 (2023).

⁷J. Forssén, "Scintillating and decorrelating signals for different propagation paths in a random medium," *Appl. Acoust.* **221**, 110038 (2024).

⁸P. Blanc-Benon, B. Lipkens, L. L. Dallois, M. F. Hamilton, and D. T. Blackstock, "Propagation of finite amplitude sound through turbulence: Modeling with geometrical acoustics and the parabolic approximation," *J. Acoust. Soc. Am.* **111**, 487–498 (2002).

⁹F. Coulouvrat, D. Luquet, and R. Marchiano, "Numerical model of sonic boom in 3D kinematic turbulence," *AIP Conf. Proc.* **1685**, 090008 (2015).

¹⁰T. A. Stout, V. W. Sparrow, and P. Blanc-Benon, "Evaluation of numerical predictions of sonic boom level variability due to atmospheric turbulence," *J. Acoust. Soc. Am.* **149**, 3250–3260 (2021).

¹¹D. K. Wilson, C. L. Pettit, V. E. Ostashev, and M. J. Kamrath, "Signal power distributions for simulated outdoor sound propagation in varying refractive conditions," *J. Acoust. Soc. Am.* **151**(6), 3895–3906 (2022).

¹²S. Bradley, *Atmospheric Acoustic Remote Sensing: Principles and Applications* (CRC Press, Boca Raton, FL, 2010).

- ¹³D. K. Wilson, C. R. Tate, D. C. Swanson, and K. M. Reichard, "Acoustic scintillations and angle-of-arrival fluctuations observed outdoors with a large planar vertical microphone array," *J. Acoust. Soc. Am.* **106**(2), L24–L29 (1999).
- ¹⁴S. L. Collier, V. E. Ostashev, C. Reiff, W. C. K. Alberts II, L. Sim, D. Tran-Luu, D. K. Wilson, and M. V. Scanlon, "Impulsive acoustic bearing estimation for ground and aerial platforms that account for the effects of atmospheric refraction and turbulence," in *Proceedings of the Military Sensing Symposium (BAMS)*, Washington, DC (October 24–28, 2011).
- ¹⁵S. L. Collier, L. I. Solomon, D. A. Ligon, M. F. Denis, J. M. Noble, W. C. K. Alberts, L. K. Sim, D. D. James, and C. G. Reiff, "Atmospheric turbulence effects on acoustic vector sensing," *Proc. Mtgs. Acoust.* **30**, 045009 (2017).
- ¹⁶S. Cheinet, M. Cosnefroy, F. Königstein, W. Rickert, M. Christoph, S. L. Collier, A. Dagallier, L. Ehrhardt, V. E. Ostashev, A. Stefanovic, T. Wessling, and D. K. Wilson, "An experimental study on the atmospheric-driven variability of impulse sounds," *J. Acoust. Soc. Am.* **144**(2), 822–840 (2018).
- ¹⁷D. K. Wilson, "Performance bounds for acoustic direction-of-arrival arrays operating in atmospheric turbulence," *J. Acoust. Soc. Am.* **103**, 1306–1319 (1998).
- ¹⁸S. L. Collier and D. K. Wilson, "Performance bounds for passive sensor arrays operating in a turbulent medium: Plane-wave analysis," *J. Acoust. Soc. Am.* **113**, 2704–2718 (2003).
- ¹⁹A. D. Wheelon, *Electromagnetic Scintillation. Vol. 1: Geometrical Optics* (Cambridge University Press, New York, 2001).
- ²⁰A. Ishimaru, *Wave Propagation and Scattering in Random Media* (IEEE Press, New York, 1997).
- ²¹A. I. Kon and V. I. Tatarskii, "Parameter fluctuations of a space-limited light beam in a turbulent atmosphere," *Izvestiya VUZ. Radiofiz.* **8**(5), 870–875 (1965).
- ²²V. E. Ostashev, S. L. Collier, and D. K. Wilson, "Transverse-longitudinal coherence function of a sound field for line-of-sight propagation in a turbulent atmosphere," *Waves Random Complex Media* **19**(4), 670–691 (2009).
- ²³M. J. Kamrath, V. E. Ostashev, D. K. Wilson, M. J. White, C. R. Hart, and A. Finn, "Vertical and slanted sound propagation in the near-ground atmosphere: Amplitude and phase fluctuations," *J. Acoust. Soc. Am.* **149**(3), 2055–2071 (2021).
- ²⁴V. E. Ostashev, M. J. Kamrath, D. K. Wilson, M. J. White, C. R. Hart, and A. Finn, "Vertical and slanted sound propagation in the near-ground atmosphere: Coherence and distributions," *J. Acoust. Soc. Am.* **150**(4), 3109–3126 (2021).
- ²⁵V. E. Ostashev, D. K. Wilson, A. Finn, and E. Barlas, "Theory for spectral broadening of narrowband signals in the atmosphere and experiment with an acoustic source onboard an unmanned aerial vehicle," *J. Acoust. Soc. Am.* **145**(6), 3703–3714 (2019).
- ²⁶V. A. Krasilnikov, "Sound propagation through a turbulent atmosphere," Ph.D. thesis, Institute Theoretical Geophysics Akad. Nauk SSSR, Moscow, 1941 (in Russian).
- ²⁷D. I. Blokhintzev, *Acoustics of a Nonhomogeneous Moving Medium* (Brown University, Providence, RI, 1956).